ARTICLE
Journal of Cellular Biochemistry 115:476–487 (2014)

Journal of Cellular Biochemistry

Nuclear Structures Surrounding Internal Lamin Invaginations

Soňa Legartová,[1] Lenka Stixová,[1] Oskar Laur,[2] Stanislav Kozubek,[1] Petra Sehnalová,[1] and Eva Bártová[1]*

[1]*Institute of Biophysics, Academy of Sciences of the Czech Republic, 612 65, Brno, Czech Republic*
[2]*Emory University School of Medicine, Emory University, Atlanta, Georgia 30322*

ABSTRACT

A- and C-type lamins are intermediate filament proteins responsible for the maintenance of nuclear shape and most likely nuclear architecture. Here, we propose that pronounced invaginations of A/C-type lamins into the nuclear interior represent channels for the transport of regulatory molecules to and from nuclear and nucleolar regions. Using fluorescent protein technology and immunofluorescence, we show that A-type lamin channels interact with several nuclear components, including fibrillarin- and UBF-positive regions of nucleoli, foci of heterochromatin protein 1 β, polycomb group bodies, and genomic regions associated with DNA repair. Similar associations were observed between A/C-type lamin channels and nuclear pores, lamin-associated protein LAP2α, and promyelocytic leukemia nuclear bodies. Interestingly, regions with high levels of A/C-type lamins had low levels of B-type lamins, and vice versa. These characteristics were observed in primary and immortalized mouse embryonic fibroblasts as well as human and mouse embryonic stem cell colonies exhibiting stem cell-specific lamin positivity. Our findings indicate that internal channels formed by nuclear lamins likely contribute to normal cellular processes through association with various nuclear and nucleolar structures. J. Cell. Biochem. 115: 476–487, 2014.

KEY WORDS: LAMINS; NUCLEAR PORES; CHROMATIN; TRANSCRIPTION; PML BODIES; DNA REPAIR; HP1 PROTEIN; ES CELLS

Lamins are structural proteins that belong to the type V intermediate filament protein family. These proteins are major components of the nuclear envelope, and laminopathy disorders are associated with abnormal nuclear envelope lobulations [Goldman et al., 2004]. In mammalian cells, A- and C-type lamins are derived by alternative splicing of the pre-mRNA template encoded by the *Lmna* gene [Lin and Worman, 1993]. Other important components of nuclear lamina are B1- and B2-type lamins, which are encoded by the distinct genes *LMNB1* and *LMNB2* [Peter et al., 1989; Vorburger et al., 1989]. It is generally accepted that lamins are associated with the inner nuclear membrane, but these proteins can also interlace with the nucleoplasm [Goldman et al., 1992; Lutz et al., 1992]. Moreover, nuclear envelope is responsible for controlling nuclear function, including gene expression, via interaction with chromatin [Malhas and Vaux, 2009]. Thus, nucleoplasmic lamins may contribute to proper nuclear functions including replication, transcription, and DNA repair [Dechat et al., 2008; Dechat et al., 2010a; Redwood et al., 2011a, 2011b]. Recent studies report that B-type lamins are static components of the nuclear interior, whereas A-type lamins are more dynamic [Tang et al., 2008; Shimi et al., 2008, reviewed in Dechat et al., 2010b]. Furthermore, Tang et al. [2008] found that A-type lamin mobility increased when the nuclear lamina contained low levels of B1-type lamin. Additional aspect that should be also taken into account is the internal position of lamins [Hozák et al., 1995] that can be components of nuclear matrix [Barboro et al., 2010]. Dimerization of internal lamins with nuclear mitotic apparatus protein (NuMa), stabilized by RNA, could determine higher-order chromatin organization [Barboro et al., 2003].

Abbreviations: BrdU, bromo-deoxyuridine; ESCs, embryonic stem cells; FISH, fluorescence in situ hybridization; FlU, fluoro-uridine; GFP, green fluorescence protein; HP1, heterochromatin protein 1; LAP2α, lamina-associated polypeptide; MEF, mouse embryonic fibroblast; ICR, imprinting control region; NB, nuclear body; Nu, nucleolus; PBS, phosphate-buffered saline; PML, promyelocytic leukemia bodies; TEM, transmission electron microscopy; UBF1, upstream binding factors 1; TSA, trichostatin A; wt, wild type; γH2AX, phosphorylated histone H2AX.

Conflict of interest: none.

Grant sponsor: Ministry of Education, Youth, and Sports of the Czech Republic; Grant number: COST-CZ LD11020.

*Correspondence to: Eva Bártová, Institute of Biophysics, Academy of Sciences of the Czech Republic, 612 65 Brno, Czech Republic. E-mail: bartova@ibp.cz

Manuscript Received: 23 July 2013; Manuscript Accepted: 23 September 2013
Accepted manuscript online in Wiley Online Library (wileyonlinelibrary.com): 7 October 2013
DOI 10.1002/jcb.24681 • © 2013 Wiley Periodicals, Inc.

The association of lamins with nuclear compartments, nuclear bodies, and chromatin has been well established. For instance, we recently showed that the nuclear trajectory of promyelocytic leukemia bodies (PMLs) is significantly influenced by A-type lamin deficiency [Stixová et al., 2012]. Moreover, the association of lamins with specific nuclear proteins, including LAP2α (LAP2β) or heterochromatin protein 1 (HP1), is fundamental for the maintenance of optimal nuclear architecture, especially the organization of chromatin [Taniura et al., 1995; Lattanzi et al., 2007; Wiesel et al., 2008]. Moreover, many authors showed that lamin B1 itself can bind chromatin [summarized by Burke and Stewart, 2013], and advanced molecular biology studies showed that Dam-lamin B1 or Dam-emerin could potentially methylate adjacent chromosomal regions that associate with other components of nuclear lamina [Burke and Stewart, 2013]. As previously mentioned, lamins may regulate transcription by interacting with chromatin domains, as evidenced by association of peripheral lamins with transcription factors. For example, regulation of Oct-1 gene transcription has been attributed to lamin B1 function. This supports the fact that lamin B deficient cells lost Oct1-lamin B1 association [Malhas et al., 2009]. In the past, however, A/C-type lamins were considered to merely provide mechanical support for the nucleus, anchoring heterochromatin to the inner nuclear membrane [summarized by Worman and Courvalin, 2004]. Importantly, loss of heterochromatin at the nuclear periphery occurs in many laminopathy disorders and is likely related to epigenetic disturbances in lamin-deficient cells. For example, cells of Hutchinson-Gilford progeria syndrome origin are characterized by low levels of histone silencing markers, including H3K9 trimethylation (me3) and H3K27me3, but high levels of H4K20me3 [Scaffidi and Misteli, 2006; Shumaker et al., 2006; Shimi et al., 2008]. A-type pre-lamins or lamins themselves are also post-translationally modified by farnesylation, carboxymethylation [summarized by Dechat et al., 2008; Reddy and Comai, 2012], phosphorylation [Ottaviano and Gerace, 1985], sumoylation [Zhang and Sarge, 2008], and ADP-ribosylation [Adolph, 1987]. Moreover, during apoptosis, B-type lamins associate with protein kinase C-δ (PKC-δ), and activation of PKC-δ by caspase 3 appears to be concomitant with B-type lamin phosphorylation and proteolysis [Cross et al., 2000].

Lamin-deficient cell nuclei are prone to morphological changes known as nuclear blebs, which contain chromatin markers, such as H3K4 methylation and RNA polymerase II, which are associated with transcriptionally active genomic regions [Shimi et al., 2008]. We recently described the presence of PML bodies in these atypical nuclear structures [Stixová et al., 2012]. Furthermore, Shimi et al. [2008] reported relocation of the gene-rich human chromosome 19, which is normally positioned deep in the nuclear interior, to nuclear blebs that are deficient in B-type lamins but positive for A/C-type lamins. These findings imply that A-type lamins associate with gene-rich domains, whereas B-type lamins preferentially make contact with gene-poor chromosomal regions. Previous experiments also confirm that rearrangement of chromatin occurs in lamin disorders, such as that observed in premature aging syndrome [Vlcek and Foisner, 2007].

From a structural point of view, the nuclear membrane is a dynamic component of the interphase nucleus that contains invaginations of nuclear envelope origin. This network of invaginations is called the nucleoplasmic reticulum (NR), and two main classes have been described: (1) type I invaginations consisting of only inner nuclear membrane components and (2) type II invaginations consisting of both inner and outer nuclear membranes and usually containing both A- and B-type lamins [summarized by Malhas and Vaux, 2011]. Interestingly, the ends of invaginated channels associate with nucleoli compartments, and B1-type lamin "speckles" are in close proximity to nucleoli or encircle nucleoli compartments [McNamara et al., 2012]. These observations led us to investigate the relationship between A–type lamin-positive invaginations and heterochromatic regions, nuclear pores, replication foci, and DNA repair-related genomic regions. Our aim was to determine the potential influence of internal channels formed by nuclear lamina on structures that play important roles in physiological nuclear processes. Moreover, we analyzed if A-type lamin positive channels associate with other components of nuclear membrane, including LAP2α.

MATERIALS AND METHODS

CELL CULTIVATION AND TREATMENT

Mouse embryonic fibroblasts (MEFs; gift from Dr. Teresa Sullivan and Dr. Collin L. Stewart from Institute of Medical Biology, Singapore; [Sullivan et al., 1999]) were cultivated in Dulbecco′s modified Eagle′s medium with 10% fetal calf serum. During cultivation, 3×10^5 cells were re-suspended in fresh medium in a new cultivation dish. Spontaneously immortalized MEFs (iMEFs) were characterized by 4–6 copies of the *Lmna* gene (Fig. S1). Based on comparisons with primary MEFs, isolated from 12.5-day-old ICR mouse embryos [Bártová et al., 2008], we determined that *Lmna* copy number increase did not substantially influence the status of A-type lamin-positive invaginations. For experiments with primary MEFs, ICR mice were bred in the Faculty of Medicine Core Facility, Masaryk University, Brno, Czech Republic. Mice were kept under standard conditions and sacrificed by overexposure to anesthetics. All procedures were approved by the National and Institutional Ethics Committee (protocol #224/2012) and were in compliance with the European Community Guidelines of accepted principles for the use of experimental animals. Primary MEFs, with normal karyotype, we used for immunofluorescence immediately after isolation, when adhered to cultivation dishes. Moreover, we standardly use these cells for cultivation of human ESCs. Cultivation of primary MEFs is well-established protocol in our laboratory.

Similar to MEFs, 3T3 cells stably expressing heterochromatin protein 1β (HP1β; gift from Dr. Paul Verbruggen (Swammerdam Institute for Life Sciences, University of Amsterdam, The Netherlands), were maintained at 37°C in a humidified atmosphere containing 5% CO_2. For microscopic observation of live cells, cell cultures were seeded on γ-irradiated 50-mm glass bottom dishes (No. 0, #P50G-0-30-F, MatTek Corporation, Ashland, MA). When cells reached 70% confluence, they were treated with a final concentration of 100 nM trichostatin A (TSA) for 24 h. For studies of DNA repair-related proteins, cells were irradiated with 5 Gy of γ-rays (Cobalt-60).

Mouse embryonic stem cells (ESCs; line D3; ATCC) and GOWT1 mESCs stably expressing GFP-OCT3/4 (gift from Dr. Hitoshi Niwa, Center for Developmental Biology, Riken, Japan) were cultivated as described by Bártová et al. [2011] and mESC differentiation was induced according to Stixová et al. [2012]. Human ESCs (hESCs; line

CCTL14; gift from Dr. Vladimír Rotrekl, Department of Biology, Faculty of Medicine, Masaryk University) were cultured as described by Holubcová et al. [2011].

MEFs were cultivated in standard in vitro conditions, on gelatine coated microscope slides, optimal growth conditions were inspected every day. Human ESCs were cultivated by the use of feeder layer of primary MEFs or on BD Matrigel™ and similar results were obtained. Human ESCs were purchased and maintained according to the Czech national law 227/2006, and Ethics Committee agreement No.: 616/2012-31.

CELL TRANSFECTION WITH PLASMID DNA

Plasmids encoding GFP-HP1β [Cheutin et al., 2003], GFP-lamin A (#17662, Addgene, Cambridge, MA; Scaffidi and Misteli [2008]), GFP-PML (gift from Roche NimbleGen, Inc., Waldkraiburg, Germany), or GFP-UBF (#17656, Addgene; Dundr et al., 2002) were used for living cell experiments. In addition, sequences encoding A-type lamins were re-cloned into a BABEpuro-mCherryETP1 vector. The plasmids of interest were introduced into *E. coli* DH5α, and DNA was isolated using the QIAGEN Plasmid Maxi Kit (#121693, QIAGEN, Bio-Consult, Czech Republic). Cells were transfected with 2–5 μg plasmid DNA using the METAFECTENE™PRO reagent according to manufacturer's instructions (Biontex Laboratories GmbH, Martinsried/Planegg, Germany).

IMMUNOFLUORESCENCE

Cells were fixed in 4% paraformaldehyde for 10 min at room temperature (RT), permeabilized with 0.2% Triton X-100 for 10 min and 0.1% saponin (Sigma–Aldrich, Prague, Czech Republic) for 12 min, and washed twice in phosphate-buffered saline (PBS) for 15 min. Bovine serum albumin (1% dissolved in PBS) was used as a blocking solution. Slides with fixed cells were washed for 15 min in PBS and incubated with the following antibodies: anti-A-type lamin (#ab26300, Abcam, Cambridge, UK), anti-A/C-type lamin (sc-7293, Santa Cruz Biotechnology, Heidelberg, Germany), anti-B-type lamin (#sc-6217, Santa Cruz Biotechnology), anti-fibrillarin (#ab5821, Abcam), anti-phosphorylated histone H2AX (γH2AX; phospho S139; #ab2893, Abcam), anti-53BP1 (#ab21083, Abcam), anti-BMI1 (05–637, Millipore, Prague, Czech Republic), anti-nuclear pore (#ab24609, Abcam), or anti-LAP2α (#ab5162, Abcam, Cambridge, UK).

BrdU AND FLU INCORPORATION

3T3 cells and MEFs were grown to 70% confluence and then incubated with 10 μM 5-bromo-2′-deoxy-uridine (BrdU) for 24 h. Cells were stained using the BrdU Labeling and Detection Kit I (#11296736001, Roche). The control for BrdU detection was performed using an appropriate antibody according to manufacturer instructions (Roche). For fluoro-uridine (FlU) incorporation, cells were incubated with FlU (Sigma–Aldrich) for 24 h and then fixed. FlU detection was performed using an antibody from the BrdU Labeling and Detection Kit I according to Kozlova et al. [2006].

DNA–FLUORESCENCE IN SITU HYBRIDIZATION (FISH) TECHNIQUES

Cells were fixed in 4% formaldehyde for 8 min at RT and then washed in PBS three times for 2 min. Cells were permeabilized using 0.1 N HCl/0.02% Triton X-100 (15 min at RT), 0.1 M Tris (pH 8; 10 min at RT), and 0.01% saponin/0.01% Triton X-100 (12 min at RT). After washing in PBS (three washes for 2 min), slides were incubated in 20% glycerol solution for 20 min at RT. Cells were sequentially treated with 70%, 80%, and 90% ethanol (cooled to −20°C), followed by freezing in liquid nitrogen three times and incubation in 50% formamide for 15 min at 75°C. Cells were then treated with 70% ethanol at RT and hybridized overnight with the *Lmna* gene-specific DNA probe, mouse clone RP24–171H19 (3qF1; Pieter de Jong's BAC/PAC Resource Center, Children's Hospital, Oakland, CA, http://bacpac.chori.org/). DNA was tagged by digoxigenin (DIG) using a DIG-nick-translation mix (Roche) and Cot-1 human DNA (Roche). DNA probes were denatured at 65–70°C for 10 min in a thermal cycler and annealed for 30–60 min at 37°C. After hybridization, preparations were washed with 50% formamide for 15 min at 43°C, 2× SSC/0.1% Tween for 8 min at 43°C, and 4× SSC/0.2% Igepal for 4 min at RT. Antibodies against DIG (Roche) or Avidin-Fluorescein (Roche) were applied for 15 min at 37°C. After washing four times in SSC/0.2% Igepal (three times for 4 min at 37°C and once for 4 min at RT), the slides were counterstained with DAPI (Sigma–Aldrich) (results of this technique are shown in Fig. S1).

CONFOCAL MICROSCOPY

Confocal microscopy was performed using a Leica TCS SP5-X system equipped with a white light laser (WLL; wavelengths 470–670 nm in 1-nm increments), argon laser (488 nm), ultraviolet lasers (405 and 355 nm), and two hybrid detectors (Leica Microsystems, Mannheim, Germany). WLL allows continuous tuning of the colours from green to dark-red through the spectrum. Thus, several fluorochromes can be visualized simultaneously and cross-talk between fluorochromes is eliminated by sequential scanning mode. For observation we used an oil objective (HCX PL APO, lambda blue) with a magnification of 63× and numerical aperture of 1.4. All of our microscopy approaches were based on a sequential scanning, we used bidirectional mode with 1,024 × 1,024 format, 400 Hz speed, eight line average, 0.772 μm z-stack thickness, and 240.5 × 240.5 nm pixel size. The white light laser was set to 85% output, and the acusto-optic tunable filter (AOTF) was set at 15% laser power when hybrid detectors were not used. When hybrid detectors were applied, 2% AOTF laser power was optimal to avoid bleaching of fluorochromes during time-lapse microscopy.

FRET (FÖRSTER RESONANCE ENERGY TRANSFER)

To determine possible interactions among proteins, we used the FRET Acceptor Photobleaching technique [Piston and Kremers, 2007]. Proteins were labeled by mCherry and GFP (or, alternatively, GFP and Alexa 594). Fluorochromes were selected based on their spectral properties to increase their efficiency as FRET donor-acceptor couples [Dinant et al., 2008]. First, excitation and emission wavelengths were set for the donor (GFP or Cy5) and then for acceptor (mCherry or Cy3). Donor fluorescence intensity was measured at the region of interest (ROI). Next, bleaching of the acceptor was performed via 100% laser power. Finally, donor fluorescence intensity was re-measured, and FRET efficiency was calculated using LEICA LAS AF software (version 2.1.2).

For FRET we used microscopy, based on the TCS Leica SP5-X imaging system, equipped with a WLL that allows to select any excitation wavelength from 470 to 670 nm in 1-nm increments. As

described by Sun et al. [2009], WLL represents an excellent tool for precise tailoring of excitation and emission characteristics of selected fluorochromes. Moreover, LEICA LAS AF software tools have ability to eliminate cross-talk between fluorochromes and enable to set exact excitation and emission conditions for both donor and acceptor, which is a main requirement for optimal FRET.

TRANSMISSION ELECTRON MICROSCOPY (TEM)

Cells were trypsinized and washed in PBS. The cell pellet was fixed for 1 h in 300 mmol/L glutaraldehyde dissolved in sodium cacodylate buffer (100 mmol/L) and an additional 3 h in fresh solution. Samples were prepared for TEM according to Galiová et al. [2008]. Cells were immersed overnight at RT in Durcupan (Durcupan™ ACM Fluka, #44611, Sigma Aldrich, Czech Republic), a water-soluble embedding medium. Sections were then incubated in Durcupan at 50°C for 4 h. Polymerization was performed at 60, 70, and 80°C for 1 day each. Ultra-thin sectioning was performed using a LEICA EM UC6 ultra-microtome. Sections were placed on grids (SPI, West Chester, PA) and incubated with 2% uranyl acetate (Pliva-Lachema a.s., Brno, Czech Republic) for 10 min and plumbic nitrate for 5 min, both in the dark. Sections were washed in double distilled water, and cells were studied using a MORGANI 268D transmission electron microscope (FEI Company, Hillsboro) equipped with a MegaView III CCD camera. Images were analyzed using Analy-SIS software (Soft Imaging System) in the core facility at the Faculty of Medicine, Masaryk University.

RESULTS

LAMIN MORPHOLOGY AND ASSOCIATION OF A-TYPE LAMIN WITH HP1β PROTEIN

TEM and fluorescence microscopy studies confirmed the presence of both A- and B-type lamins in the nuclear interior, which manifested as lamina invaginations (summarized by Malhas and Vaux, 2011) (Fig. 1A and B). In iMEFs, internal B-type lamins often associated with clusters of centromeric heterochromatin called chromocenters (densely stained with DAPI in Fig. 1A: b or see red arrows in Fig. 1A: d from TEM). Very long protrusions of nuclear lamina inside the nuclear interior were observed when nuclei were visualized by TEM (Fig. 1A: c,d) or when MEFs were transfected with plasmid DNA encoding mCherry-lamin A (Fig. 1B: a,b). These nuclear channels invaded the nuclear interior, and channel length was approximately 30% of the nuclear radius (Fig. 1B: c). Invaginations positive for A-type lamins were associated with GFP-HP1β foci and were visible in both two- (2D) and three-dimensional (3D) projections (Fig. 2A: a–c or B). For explanation, lateral visualization of 3D projections depended on setting of the projection cross; for example, in Figure 2A: c, cross shows association of lamins with HP1β in x–z and y–z modes). The highest level of A-type lamins was found on the lateral sides of nuclei and where cells attached to the cultivation dish (yellow frame in Fig. 2A: c shows lateral side or Fig. 2C: a represents A-type lamin morphology at the region where the cell attached cultivation surface). Whereas a lower level of A-type lamins was found on the sides of nuclei where cells were not attached to the cultivation dish (yellow arrows in Fig. 2A: b,c).

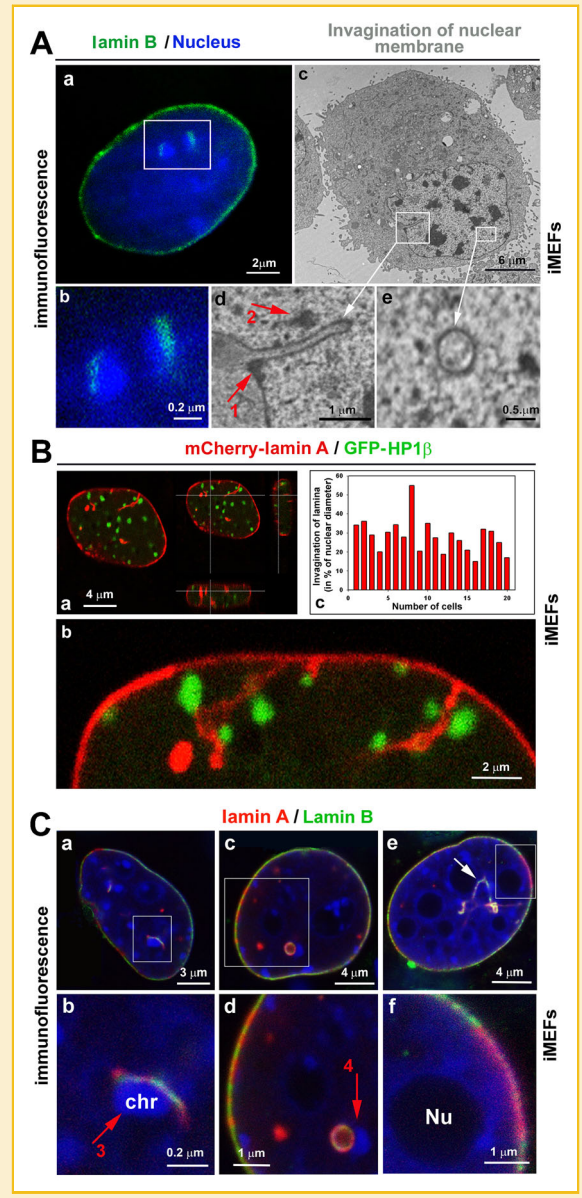

Fig. 1. Visualization of lamin morphology and invagination in iMEF nuclei. A: Visualization of B1-type lamin in MEFs (green) confirmed an abundance of this lamin type at the nuclear periphery and interior (a,b). Internal lamins were surrounded by clusters of centromeric heterochromatin called chromocenters [densely stained by DAPI in (b); red arrows in (d)]. Invagination of nuclear lamina into the nuclear interior was confirmed by TEM (c–e). B: (a,b) Mouse 3T3 cells stably expressing GFP-HP1β (green) were transfected with plasmid encoding mCherry-tagged A/C-type lamins (red). HP1β foci were found in proximity to invaginated nuclear channels. Visualization of A/C-type lamin lateral projections depended on cross settings in the selected ROI. Observation was performed in living cells. B: (c) Length of A-type lamin channels shown as a percentage of maximum nuclear diameter (number of cells = 20). C: Double immunostaining of A-type (red) and B-type (green) lamins in iMEF interphase nuclei (blue). Nu, nucleolus; chr, chromocenter (shown by red arrows). Scale bars are shown in each panel: Aa (2 μm); Ab (0.2 μm); Ac (6 μm); Ad (1 μm); Ae (0.5 μm); Ba (4 μm); Bb (2 μm); Ca (3 μm); Cb (0.2 μm); Cc (4 μm); Cd (1 μm); Ce (4 μm); Cf (1 μm). In panels Aa, Ab, Ca–f, DAPI was used for staining of nuclear DNA.

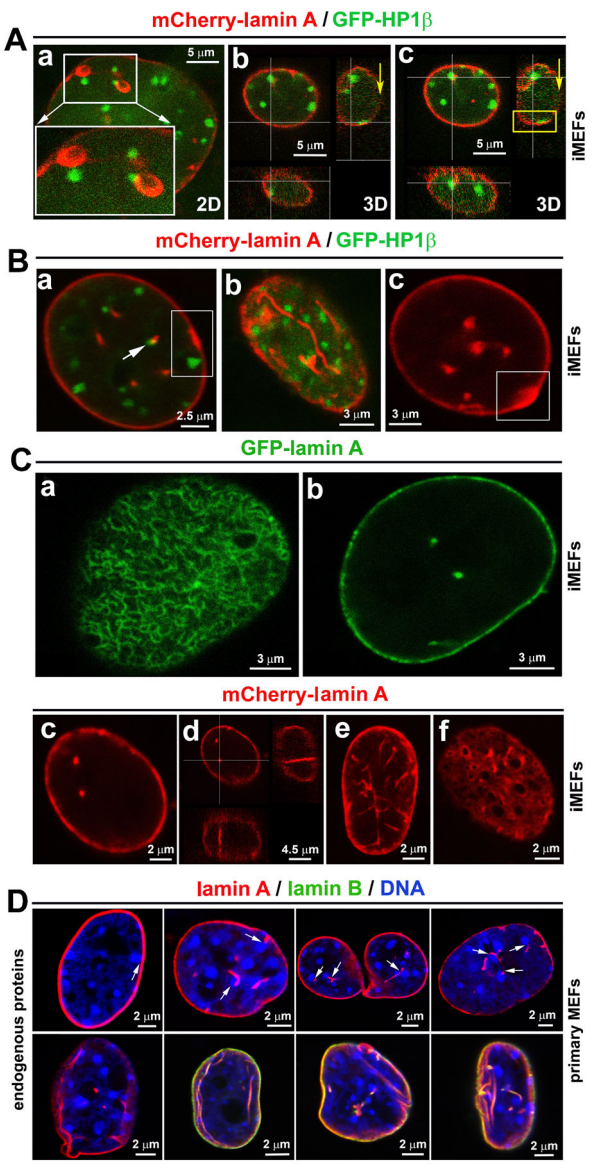

Fig. 2. Spatial association between A-type lamins and HP1β. A: (a–c) 3T3 cells stably expressing GFP-HP1β (green) and transiently expressing mCherry-lamin A (red) were visualized in 3D mode. HP1β foci were observed at both the nuclear periphery and interior. B: (a–c) Several internal A/C-type lamin foci overlapped with HP1β foci [arrow in (a)]. In some cells, increased levels of A/C-type lamins were observed at the nuclear periphery [white frames in (a) and (c)] and were associated with the formation of nuclear blebs [white frame in (c)]. The nuclear interior was interlaced with A-type lamin channels (b). C: A/C-type lamins-tagged by GFP (green) formed (a) a mesh-like structure where cells attached to cultivation dishes, but confocal microscopy showed that (b) internal lamins appeared as foci or speckles in midsections of cells. This specific morphology of A-type lamins was also evident in living iMEFs, visualized by over-expression of mCherry-lamin A (c–f). D: A- and B-type lamins in primary MEFs. Arrows show association of internal lamins with chromocenters. Scale bars are presented in each panel: Aa–c (5 μm); Ba (2.5 μm); Bb–c and Ca–b (3 μm); Cc (2 μm); Cd (4.5 μm); Ce–f (2 μm); D (2 μm). In panel D, DAPI was used for staining of nuclear DNA. Observation was performed in living cells (panels A–C).

We also observed lamin-positive invaginations by immunodetection with specific antibodies (Fig. 1C). Interestingly, nuclear regions with high levels of A-type lamins had low levels of B-type lamins, and vice versa (see chain-like morphology in Fig. 1C, particularly 1C: d,f). These analyses also confirmed following characteristics specific to lamin-positive compartments: (1) lamin channels surround internally-positioned chromocenters (Fig. 1C: b); (2) internal lamins that appear as speckles in x–y projections appear as invaginations in x–z or y–z projections (Fig. 2C: d—projection cross was set to a given lamins' "speckle" so that it appeared as a circle in planar (x-y) projections; see also Figs. 1A: e and C: c,d); (3) lamin channels were associated with nucleoli (white arrow in Fig. 1C: e).

HP1β foci and A-type lamin channels were observed in both the nuclear periphery and interior (Fig. 2A and B). In some cases, the highest levels of A-type lamins were observed within the nuclear membrane and appeared to be associated with the formation of nuclear blebs (Fig. 2B: a,c, white frames). In other cases, nuclear channels positive for A-type lamins were observed throughout the entire nuclear interior (Fig. 2B: b). Visualization of exogenous A-type lamins in living cells by both GFP and mCherry revealed dense, mesh-like structures where cells attached to the cultivation dishes (Fig. 2C: a,f). Confocal microscopy of cell midsections revealed small internal speckles (Fig. 2C: b) that in 3D projections appeared as invaginated channels, which could intersect the entire nuclear interior and enter the most central regions of interphase nuclei (Fig. 2C: d,e). Internal lamins and A-type lamin channels were also associated with chromocenters in primary MEFs (white arrows in Fig. 2D). In these cells, morphology of A-type lamins is shown in various confocal sections. Mid-section (the first upper-left panel) mostly shows perfect A-type lamin positive nuclear rim, but in direction to attachment region, lamina invaginations also appear in primary MEFs (Fig. 2D; bottom panels). Moreover, in both iMEFs and primary MEFs, it was approximately 20% chromocenters that appeared in proximity to A/C lamin-positive channels, and many chromocenters attached peripheral lamins (Fig. 2D). We are aware that an increase density of lamin channels can be caused by lamin over-expression (Fig. 2C: a,f), but this experimental approach increased the opportunity to observe a link between lamin channels and other nuclear domains in detail; in living cells.

Here, we also observed HP1β foci in nuclear blebs, and their distribution was unaffected by treatment of cells with the histone deacetylase (HDAC) inhibitor TSA, which caused pronounced nuclear blebbing. Hyperacetylation caused by HDAC inhibition was associated with chromatin relaxation [Bártová et al., 2005], which changed the morphology of A-type lamin invaginations into the nuclear interior (compare Fig. 3A: a with Fig. 3B and C; Galiová et al., 2008). After TSA treatment small HP1β foci surround multiple A-type lamin positive internal channels (Fig. 3B, yellow frame). In non-treated cells, time-lapse confocal microscopy showed that the morphology of lamin invaginations was stable across time, but only fluorescence intensity was reduced by laser exposure (Fig. 3D; 3h-observation). This result is consistent with observation of Broers et al. [1999] showing stability of branching intra- and trans-nuclear tubular, lamin-positive, structures. Here, internal lamin channels protruded from the region where the cells attach cultivation surface (Figs. 2C: d and 3D). From the view of protein nuclear pattern we have analyzed

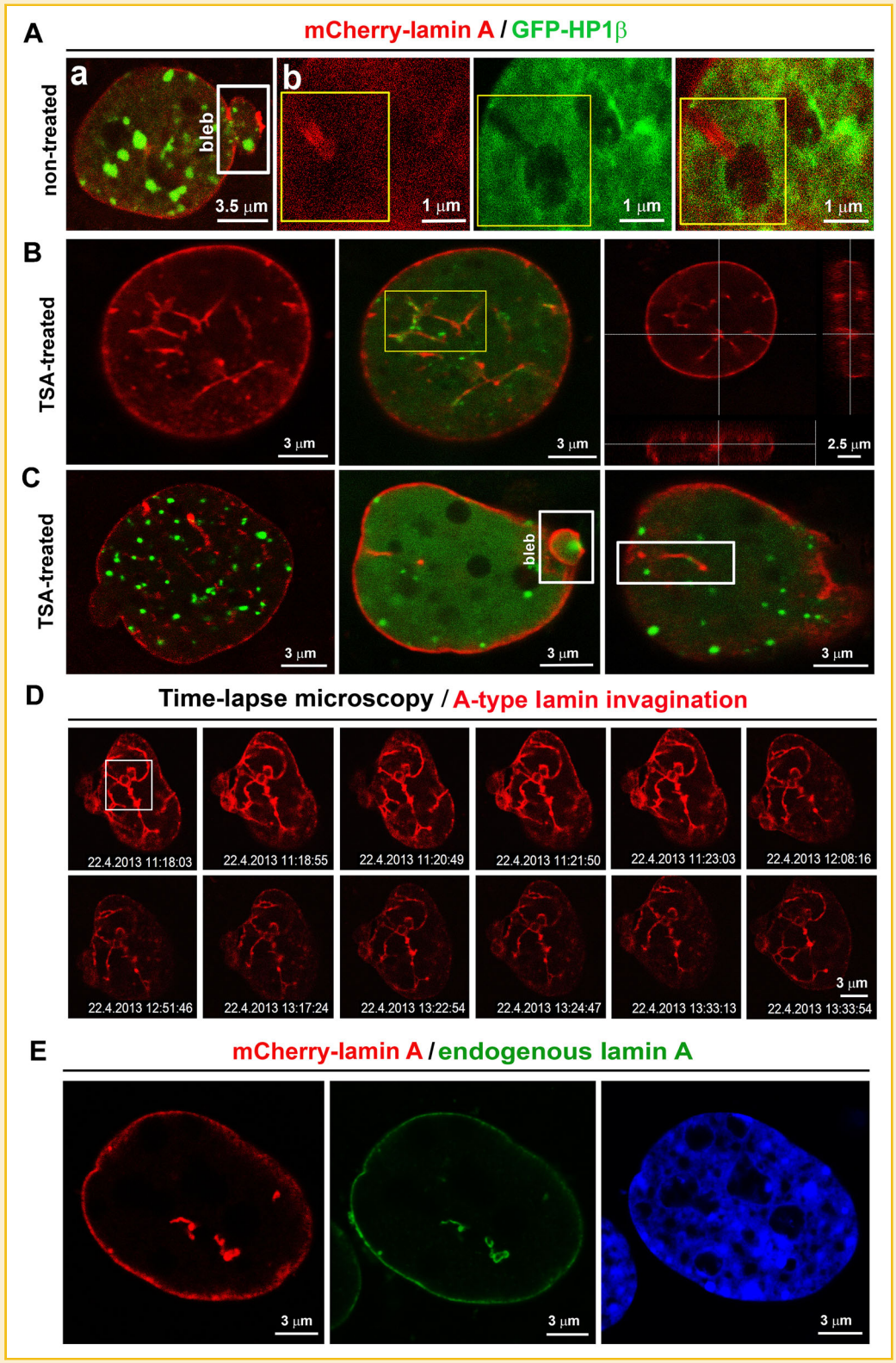

Fig. 3. A-type lamins and HP1β after HDAC inhibitor-induced hyperacetylation. A: Nuclear blebs formed spontaneously or after treatment with the HDAC inhibitor TSA. Blebs were positive for HP1β (green) (a). Channels positive for A/C-type lamins (red) directed towards nucleoli were positioned within the nuclear interior [empty space in nucleus, (b); yellow frames show A-type lamin positivity (red) in nuclear channels]. B: TSA treatment highlighted the mesh-like structure of internal lamins and did not abrogate contact between internal lamins and HP1β foci that were smaller after HDACi [yellow frame in (B)]. C: Nuclear blebs positive for A/C-type lamins contained HP1β foci after TSA treatment. D: Results of time-lapse confocal microscopy demonstrated stability of A-type lamin invaginations across time (3 h of observation). E: Morphology of endogenous (green) and exogenous (red) A-type lamins. Scale bars are shown in each panel: Aa (3.5 μm); Ab (1 μm); B–E (3 μm). In panel E, DAPI was used for staining of nuclear DNA. Observation was performed in living cells (panels A–D).

cell attachment region in Bártová et al. [2007] and we observed specific pattern of HP1α and HP1β in this region. The same trend we found here for A-type lamins, which morphology was not substantially changed over time (Figs. 2C: a,f, and 3D; Broers et al., 1999). Stable morphology seems to be also true for endogenous A-type lamin channels, which nuclear pattern was similar as internal lamins, visualized as mCherry-tagged lamin A (Fig. 3E).

Here, we additionally showed that internal lamins are associated with nucleoli compartments (Fig. 4A: a–d). Previously the same was demonstrated by McNamara et al. [2012] for "foci" of internal B1-type lamin. Here, we found that A-type lamins form invaginations oriented toward internally positioned nucleoli (see channel in yellow frames in panels of Fig. 3A: b). A/C-type lamin channels were often in close contact with fibrillarin-positive regions of nucleoli (magnification in Fig. 4A: b1 and c1; image in Fig. 4A: d is shown as separated RGB images as Fig. 4A: d1–d3).

A-TYPE LAMIN INVAGINATIONS AND REGIONS OF REPLICATION, TRANSCRIPTION, AND DNA REPAIR

We next examined the association between A-type lamins and DNA repair markers, BrdU-positive replication foci, and FlU-positive sites of active transcription (Fig. 4B and C). Internal A-type lamin channels were tightly associated with γH2AX-positive DNA lesions induced by γ-radiation (Fig. 4B: a). Similarly, peripheral A-type lamins were in proximity to γH2AX foci (Fig. 4B: b,c). Channels positive for A/C-type lamins also associated with 53BP1, another DNA repair-related protein (Fig. 4C: a,b).

Internal lamin channels did not co-localize with internally positioned BrdU-positive replication foci, but a close association between A/C-type lamins and BrdU-positive signals was found at the nuclear periphery (white frames in Fig. 4C: c,d). This association of A/C-type lamins with likely late-replicating foci is consistent with the fact that the nuclear periphery represents important region for the anchoring of heterochromatin.

We also found that internal A/C-type lamin channels were interconnected with sites of transcription marked by FlU-positive signals (Fig. 4C: e). Similar associations were found between internal A/C-type lamins channels and repressive complexes, including BMI1-positive Polycomb group proteins-related bodies (PcG; Fig. 4C: f). Moreover, internal A-type lamin channels were associated with some promyelocytic leukemia nuclear bodies (PML-NBs) and were directed to UBF-positive compartment of nucleoli (Fig. 5A and B: a–c). Furthermore, we examined the association between internal A-type lamins and nuclear pore complexes to determine whether internal lamins are membrane-bound. In many cases, immunofluorescence signals demonstrated an association between nuclear pores and internal A/C-type lamins (Fig. 5C). Moreover, internal A-type lamin channels were associated with LAP2α (Fig. 5D). These data imply that there are two types of internal lamins: (a) membrane less and (b) membrane-associated.

To investigate the potential interactions between A-type lamins and other proteins of interest, we used the FRET technique to test for relationships between A-type lamins and LAP2α or HP1β. As expected, a high FRET efficiency (43.6 ± 13.5%) was found for A-type lamins and LAP2α (Fig. 6A). However, FRET efficiency was lower for A-type lamins and HP1β at both the nuclear periphery (25.2 ± 15.8%)

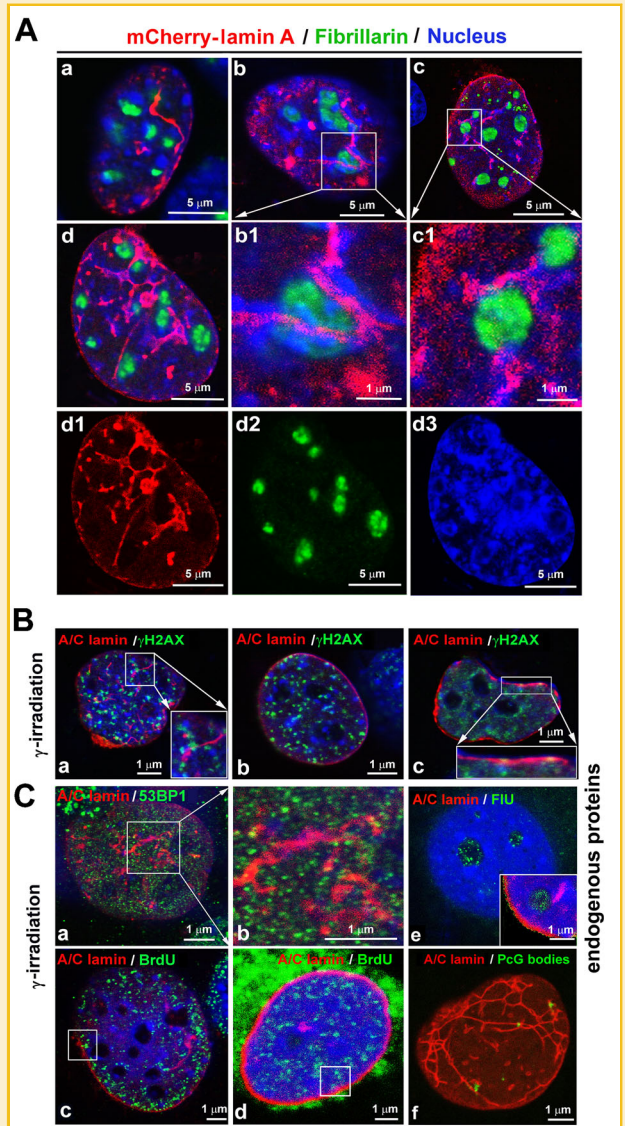

Fig. 4. Association of A-type lamins with nucleoli, DNA repair sites, and replication foci. A: Invaginated A/C-type lamin channels (red) were directed toward fibrillarin-positive nucleoli regions (green) (a–d). Magnification of ROIs in (b) and (c) are shown in (b1) and (c1), respectively; cell in (d) is shown in as separated RGB images in (d1–d3). mCherry-tagged A/C-type lamin channels surrounded or intersected fibrillarin-positive nucleoli compartments. B: (a–c) After γ-irradiation, A-type lamins were associated with γH2AX-positive genomic regions (a), and γH2AX was integrated into nuclear envelopes that were positive for A/C-type lamins (b,c). C: (a,b) 53BP1-positive foci (green) were associated with internal channels positive for A-type lamins (red). C: (c,d) Association of BrdU-positive signals (green) with A-type lamins (red) was observed at the nuclear periphery but not the nuclear interior. C: (e) FlU positivity (green) within nucleoli was associated with A/C-type lamin channels directed toward nucleoli (red). C: (f) Co-localization of PcG bodies containing BMI1 protein (green) and internal A/C-type lamin channels (red). In B–C, images show results of immunofluorescence and not transgenic expression of fluorescently labeled proteins. Scale bars are shown in each panel: Aa–d and d1–d3 (5 μm); Ab1 and Ac1 (1 μm); B–C (1 μm). In panels Aa–d, b1, c1, d3 and panels B and Ca–e, DAPI was used for staining of nuclear DNA.

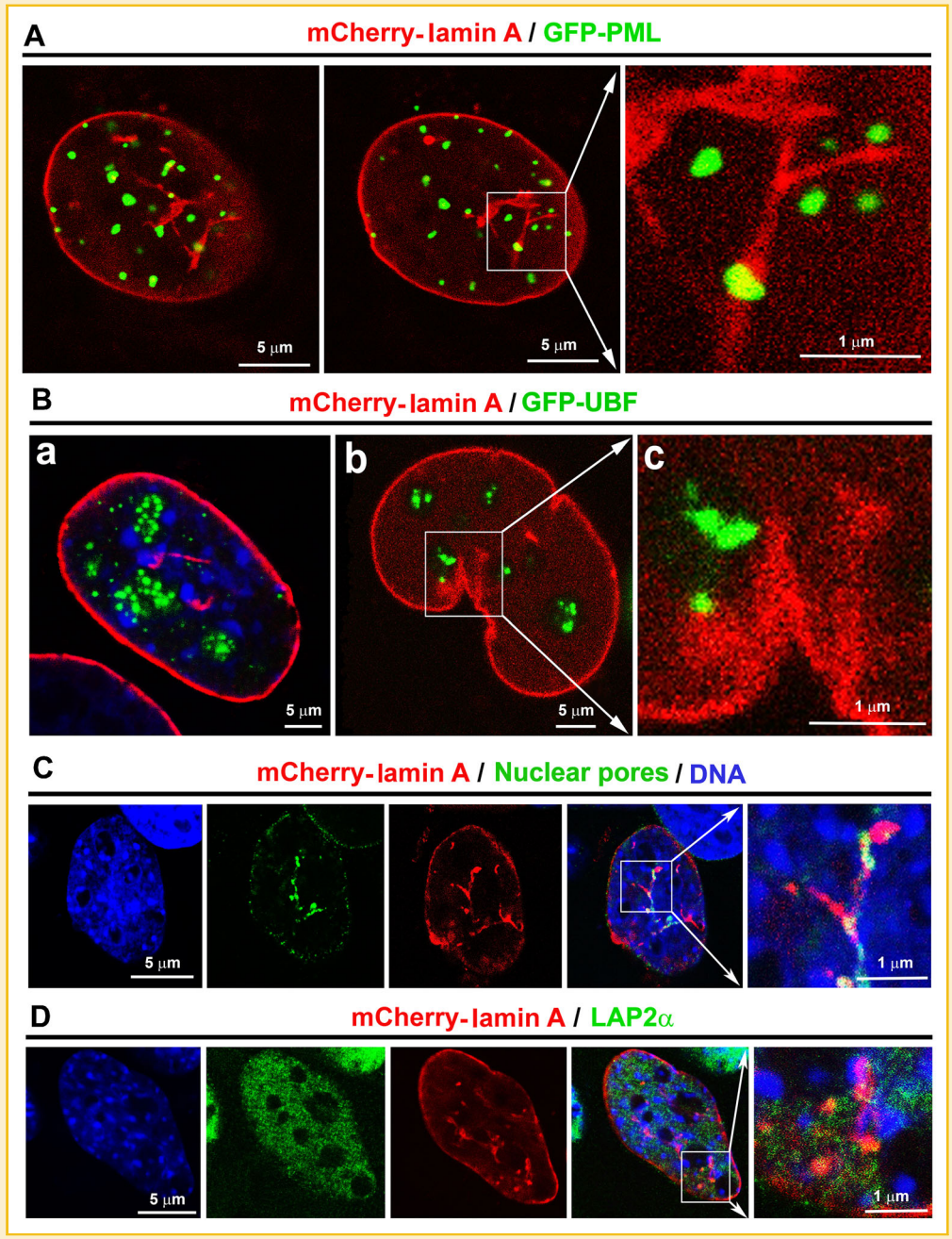

Fig. 5. Relationship between A/C-type lamins and selected nuclear proteins. A: Several PML nuclear bodies (green) strictly co-localized with internal A/C-type lamin channels (red). B: (a) UBF-positive nucleoli regions (green) were detected in proximity to A/C-type lamins (red). B: (b) UBF-positive regions also appeared near A/C-type lamins at the nuclear periphery. B: (c) Magnified frame in panel Bb showing relationship between UBF and lamins. C: Association of A/C-type lamins (red) with nuclear pores (green). D: Association of A/C-type lamins (red) with LAP2α (green). Scale bars are shown in each panel: A–D (5 μm); magnifications 1 μm. In panels Ba, C and D, DAPI was used for staining of nuclear DNA. Observation was performed in living cells (panels A, Bb, Bc).

and internal channels (18.5 ± 16.6%) (Fig. 6B: a,b; see Fig. 6C for summary). As these results indicate a rather poor interaction between A-type lamins and HP1β, the association between these proteins could be ascribed to heterochromatinization processes occurring in proximity to nuclear lamina and around nucleoli that are often surrounded by internal lamins (Fig. 6B).

Taken together, these findings suggest that internal lamins are structurally and functionally significant due to their association with several different nuclear bodies and domains. Lamin-positive nuclear compartments were associated with regions containing proteins that regulate replication, transcription, and DNA repair. A-type lamin invaginations, therefore, could potentially serve as scaffolds that

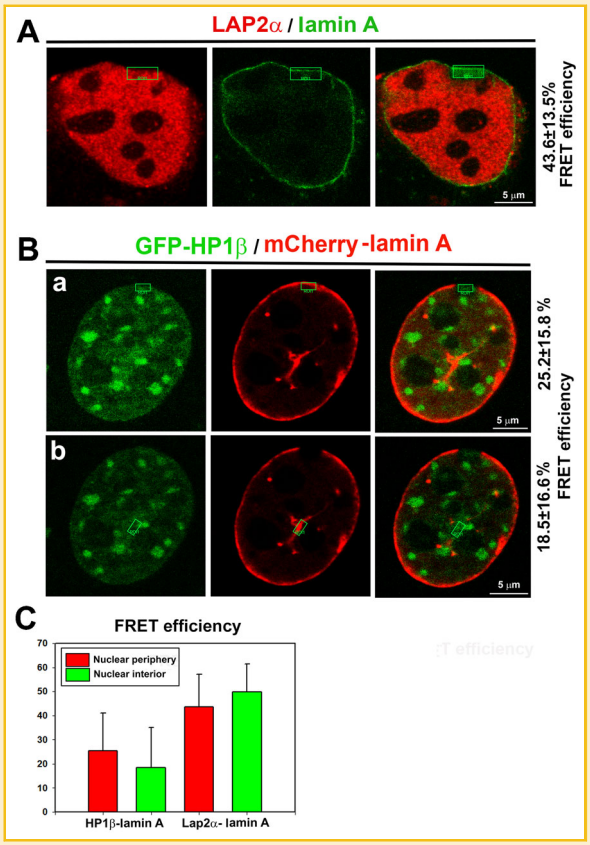

Fig. 6. FRET analysis of protein interactions. A: FRET analysis of interaction between A-type lamins (green) and LAP2α (red) (results of two independent experiments are shown, number of measurement: n1 = 14; n2 = 10). B: FRET analysis of potential interaction between (a) A-type lamins (red) and HP1β (green) at the nuclear periphery or (b) A-type lamins (red) and HP1β (green) in the nuclear interior. Scale bars are shown in each panel: A–B (5 μm). C: Summary of FRET efficiency for selected proteins. Data are shown as mean FRET efficiency (%) ± standard error of the mean. Results of two independent experiments were summarized (number of measurement: n1 = 23; n2 = 11). In panel B observation was performed in fixed cells.

influence nuclear architecture. Furthermore, A-type lamin channels could have a vital role in the transport of regulatory molecules to their biological targets.

MORPHOLOGY OF A/C- AND B-TYPE LAMINS IN EMBRYONIC STEM CELLS

We also investigated the morphology of A- and B-type lamins in embryonic stem cells, which possess de-condensed chromatin structures and therefore differ from their differentiated counterparts. In pluripotent mouse ESCs (mESCs; line D3), ~10–15% of cells in the colony were positive for A/C-type lamins (Fig. 7A: a). However, in human ESCs (hESCs; line CCTL14), cells positive for A/C-type lamins were rare (up to 5%; Fig. 7B: a, white frame labeled hESCs). By contrast, high levels of A/C-type lamin positivity were found in MEFs, which were used as a feeder layer for hESC cultivation (Fig. 7B: a, white frame labeled MEFs). Interestingly, there was no preferential location of cells positive for A/C-type lamins within ESC colonies

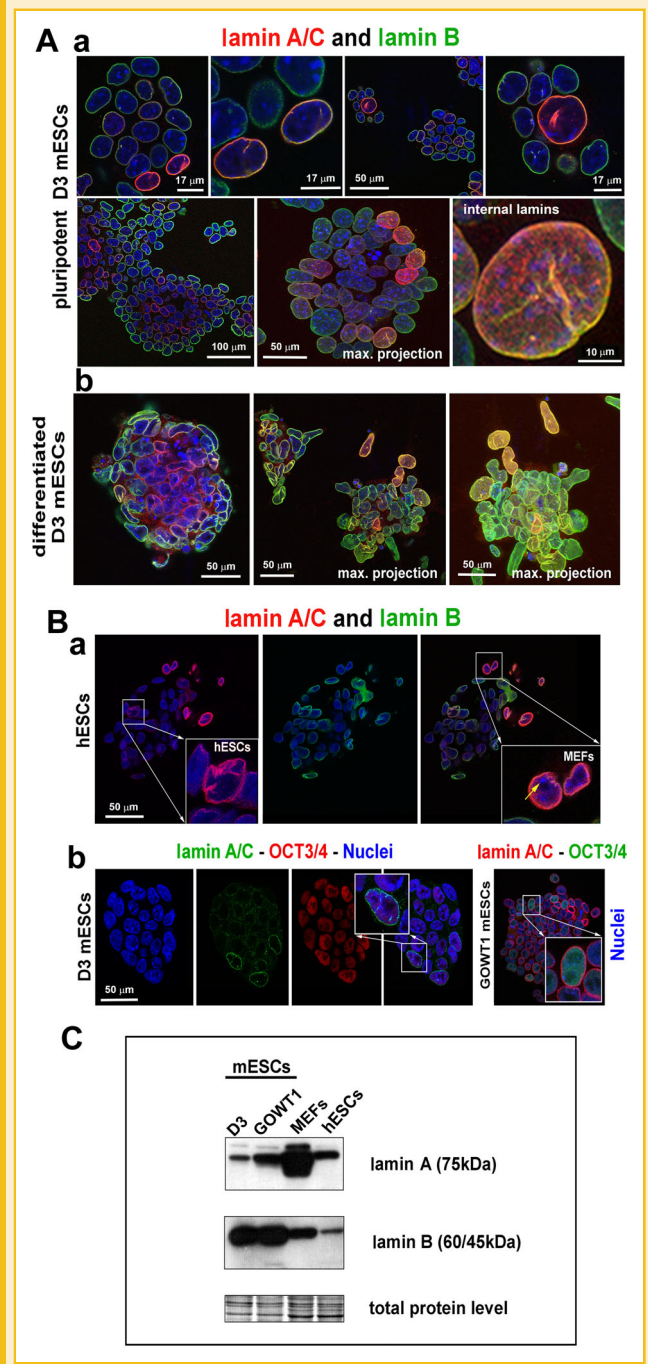

Fig. 7. A- and B-type lamins visualized by immunofluorescence and confocal microscopy in ESCs. A: A/C-type (red) and B-type (green) lamins within colonies of (a) pluripotent and (b) differentiated D3 mESCs. B: (a) A/C-type (red) and B-type (green) lamins within colonies of pluripotent hESCs. hESCs can be distinguished from MEFs (feeder layer) by chromocenters visualized by DAPI staining (yellow arrow). Example and magnification (white frames) of a hESC with a A/C-type lamin signal and MEFs that were highly positive for A/C-type lamins. B: (a) A/C-type lamin positivity and OCT3/4 level in D3 and GOWT1 mESCs. Scale bars are shown in each panel: Aa (10, 17, 50, and 100 μm); Ab (50 μm); Ba–Bb (50 μm). C: Western blots showing A- and B-type lamin levels in D3 mESCs, GOWT1 mESCs, MEFs, and hESCs. Data are normalized to total protein levels. In panels Aa, b and Ba, b, DAPI was used for staining of nuclear DNA.

(Fig. 7A: a) at a difference of what was previously found for other markers such as Nanog and H3K27me3 (i.e., Nanog-positive cells predominately in the colony interior, H3K27me3-positive cells predominately in nuclei of peripherally positioned cells; Šustáčková et al., 2012). A/C-type lamin positivity in pluripotent mESCs was not a consequence of spontaneous differentiation appearing during cultivation, because high levels of A/C-type lamin positivity were observed in GOWT1 mESCs that stably express OCT3/4. For explanation, panels in Figure 7B: b show high endogenous and exogenous OCT3/4 levels, simultaneously as lamin positivity in mESCs. As expected, differentiation of mESCs was accompanied by increased levels of A/C-type lamins, as shown by immunofluorescence (Fig. 7A: b) and western blots [Stixová et al., 2012]. Oct4 level was decreased during ESC differentiation [Stixová et al., 2012]. In comparison with MEFs, levels of A-type lamins were lower in D3 mESCs, hESCs, and GOWT1 mESCs (Fig. 7C), which is largely consistent with the findings of Constantinescu et al. [2006]. Furthermore, in comparison with mESCs and MEFs, human ESCs that we tested exhibited very low levels of B-type lamins (Fig. 7C). Invagination of lamins into nuclear interior was observed in both mESCs and hESCs (Fig. 7A: a, labeled as internal lamins; and Fig. 7B: a, labeled as hESCs).

DISCUSSION

The nuclear lamina provides structural support for the nucleus and can be considered part of the nucleoskeleton for nuclear chromatin architecture. The lamina consists of several proteins, including A- and B-type lamins, which occupy the nuclear envelope. Here, we show that invaginations of A-type lamins initiate from the mesh-like arrangement of lamins where cells attach to the cultivation dishes (Fig. 2C: a,f) and that these nuclear channels penetrate into the nuclear interior. Similar to the B1-type lamin speckles described by McNamara et al. [2012], A-type lamin channels also look like speckles in midsections of the cell studied by confocal microscopy (compare Fig. 2C: c with d). Thus, both B1- and A/C-type lamins form speckle-like structures that are associated with nucleoli compartments (Fig. 4A; McNamara et al., 2012). Additional analyses, however, revealed that A-type lamins form channels that directly interlace with fibrillarin-positive regions of nucleoli or they are oriented towards UBF1-positive nucleolar compartments, which are considered regions of active transcription of ribosomal genes (Figs. 4A and 5B). Furthermore, after γ-irradiation, A-type lamins interlaced with DNA damage markers, including γH2AX- and 53BP1-positive foci, confirming a link between lamin function and DNA repair [Redwood et al., 2011a, 2011b] (Fig. 4B, C).

We also investigated the relationship between A-type lamins and heterochromatin protein HP1β, as laminopathy disorders are not only associated with defective nuclear envelopes but may also involve re-organization of heterochromatin [Nikolova et al., 2004]. For example, heterochromatin rearrangement in laminopathic cells can manifest as HP1β morphological changes [Galiová et al., 2008; Chaturvedi and Parnaik, 2010]. Here, we confirmed the relationship between lamin and HP1β proteins by observing that internal A/C-type lamin foci and channels are surrounded by HP1β foci (Fig. 1B: b) and that there is a tight spatial relationship between lamins and some chromocenters (Figs. 1A: b, C: b, and 2D). Based on FRET analysis (Fig. 6), we conclude that the association between A-type lamins and HP1β reflects processes of heterochromatinization that most of all occur around nucleoli and in proximity to nuclear periphery, especially during cell differentiation.

Another interesting phenomenon with respect to nuclear lamina is the formation of nuclear blebs as a result of laminopathy disorders. This morphological change causes re-arrangement of the normal nuclear distribution of chromosomal territories [Meaburn and Misteli, 2007; Shimi et al., 2008]. For example, in lamin-deficient cells, guanine-cytosine-rich human chromosome 19, which is typically located in the nuclear interior, is re-located to the periphery near nuclear blebs [Shimi et al., 2008]. Laminopathy-related nuclear blebs are also characterized by the appearance of markers associated with transcriptionally active chromatin (e.g., H3K4 methylation or RNA pol II) [Shimi et al., 2008]. We recently showed that PML nuclear bodies occupy bulges of the nuclear envelope [Stixová et al., 2012] and here, we additionally documented that some PML bodies associate with tubular invaginations of nuclear lamina (Fig. 5A). Furthermore, we also observed heterochromatin foci of HP1β in nuclear blebs occurring either spontaneously or after HDAC inhibition in MEFs (Fig. 3A–C). This observation confirms a link between lamins and sub-types of HP1, which show altered levels in cells with mutation in *Lmna* gene [Scaffidi and Misteli, 2008]. Moreover, mislocalized lamins induced ubiquitin-mediated proteasomal degradation of HP1 isoforms, which also support a link between function of lamins and HP1 protein [Chaturvedi and Parnaik, 2010].

Changes in the levels of A-type lamins also accompany the differentiation of ESCs [Constantinescu et al., 2006]. Intriguingly, *Lmna* gene expression is activated during differentiation of hESCs even before down-regulation of the pluripotency factor OCT3/4. Here, we observed cells positive for A/C-type lamins in colonies of mESCs and to a lesser extent in hESCs (Fig. 7A: a and B: a,b). As expected, the level of lamins significantly increased during mESC differentiation (Fig. 7A: b; Stixová et al. [2012]). These observations confirm the importance of lamins in normal physiological processes, including cell differentiation. Moreover, our results unambiguously indicate that in the majority of cases, nuclear patterns of protein expression in ESCs must be analyzed for the entire ESC colony and not at the single-cell level, as individual ESCs may exhibit different nuclear patterns of protein expression within a single colony (Fig. 7A: a; Šustáčková et al., 2012).

Taken together, our findings indicate that A-type lamin invaginations are functionally significant channels that may serve to transport of regulatory molecules in and out of the cell nucleus. Thus, lamin channels represent important components of nuclear structure and could support the function of interchromatin compartment (IC) which is likely visible as unmarked regions in living cells stably expressing core histones, tagged by fluorescent proteins (see example in Orlova et al., 2012). This suggestion did not exclude an existence of chromatin intermingling as described by Branco and Pombo [2006], because chromatin could intermingle in proximity to lamin channels. Most of all, our observation contribute to the model of chromosome territory-interchromatin compartment

(CT-IC), which is necessary for the transport of regulatory molecules to their nuclear targets [Cremer and Cremer, 2001, 2010], because lamin channels, similarly as IC, harbor variety of functionally important non-chromatin foci or domains (Figs. 2A, 4, 5 and for IC summarized by Cremer and Cremer, 2010]. For example, in living cells, many HP1β foci, PML and PcG bodies were adjacent or co-localized with A-type lamin channels (Figs. 1B: b, 4C: f, and 5A). Moreover, 3D projections of confocal microscopy sections showed that lamin invaginations start at nuclear periphery and interlace with the nuclear interior (Fig. 2B: b and C: d). This is consistent with 3D-reconstruction of lamin morphology in interphase nuclei as published by Broers et al. [1999]. These invaginations were observed in both primary and immortalized MEFs and, to a lesser extent, in pluripotent non-differentiated ESCs (Figs. 1, 2, and 7). According to this observation, interior nuclear compartments could have, in certain extent, a direct contact with the nuclear periphery via lamin channels. Thus, hypothesis on internal nuclear network of robust channels, independent on structural framework of chromatin, must be also taken into account [Razin and Gromova, 1995]. However, here we observed many HP1β foci in proximity to A-type lamin channels, which implies that HP1β-dense heterochromatin could anchor lamin channels. This fits well with a current consensus showing the existence of dynamic lamin-associated nucleoskeleton involved in structural and functional organization of the cell nucleus [Hozák et al., 1995; Neri et al., 1999; Barboro et al., 2002; Simon and Wilson, 2011].

ACKNOWLEDGMENTS

This work was supported by the Ministry of Education, Youth, and Sports of the Czech Republic (project COST-CZ LD11020). Grant Agency of Czech Republic, projects P302/10/1022 and P302/12/G157 and Education for Competitiveness Operational Program (ECOP), CZ.1.07/2.3.00/30.0030.

REFERENCES

Adolph KW. 1987. ADPribosylation of nuclear proteins labeled with [3H] adenosine: Changes during the HeLa cycle. Biochim Biophys Acta 909:222–230.

Barboro P, D′Arrigo C, Diaspro A, Mormino M, Alberti I, Parodi S, Patrone E, Balbi C. 2002. Unraveling the organization of the internal nuclear matrix: RNA-dependent anchoring of NuMA to a lamin scaffold. Exp Cell Res 279:202–218.

Barboro P, D′Arrigo C, Mormino M, Coradeghini R, Parodi S, Patrone E, Balbi C. 2003. An intranuclear frame for chromatin compartmentalization and higher-order folding. J Cell Biochem 88:113–120.

Barboro P, D′Arrigo C, Repaci E, Patrone E, Balbi C. 2010. Organization of the lamin scaffold in the internal nuclear matrix of normal and transformed hepatocytes. Exp Cell Res 316:992–1001.

Bártová E, Pacherník J, Harničarová A, Kovařík A, Kovaříková M, Hofmanová J, Skalníková M, Kozubek M, Kozubek S. 2005. Nuclear levels and patterns of histone H3 modification and HP1 proteins after inhibition of histone deacetylases. J Cell Sci 118:5035–5046.

Bártová E, Pacherník J, Kozubík A, Kozubek S. 2007. Differentiation-specific association of HP1alpha and HP1beta with chromocentres is correlated with clustering of TIF1beta at these sites. Histochem Cell Biol 127:375–388.

Bártová E, Krejčí J, Harničarová A, Kozubek S. 2008. Differentiation of human embryonic stem cells induces condensation of chromosome territories and formation of heterochromatin protein 1 foci. Differentiation 76:24–32.

Bártová E, Šustáčková G, Stixová L, Kozubek S, Legartová S, Foltánková V. 2011. Recruitment of Oct4 protein to UV-damaged chromatin in embryonic stem cells. PLoS ONE 6:e27281.

Branco MR, Pombo A. 2006. Intermingling of chromosome territories in interphase suggests role in translocations and transcription-dependent associations. PLoS Biol 4:e138.

Broers JL, Machiels BM, van Eys GJ, Kuijpers HJ, Manders EM, van Driel R, Ramaekers FC. 1999. Dynamics of the nuclear lamina as monitored by GFP-tagged A-type lamins. J Cell Sci 112:3463–3475.

Burke B, Stewart CL. 2013. The nuclear lamins: Flexibility in function. Nat Rev Mol Cell Biol 14:13–24.

Chaturvedi P, Parnaik VK. 2010. Lamin A rod domain mutants target heterochromatin protein 1alpha and beta for proteasomal degradation by activation of F-box protein FBXW10. PLoS ONE 5:e10620.

Cheutin T, McNairn AJ, Jenuwein T, Gilbert DM, Singh PB, Misteli T. 2003. Maintenance of stable heterochromatin domains by dynamic HP1 binding. Science 299:721–725.

Constantinescu D, Gray HL, Sammak PJ, Schatten GP, Csoka AB. 2006. Lamin A/C expression is a marker of mouse and human embryonic stem cell differentiation. Stem Cells 24:177–185.

Cremer T, Cremer C. 2001. Chromosome territories, nuclear architecture and gene regulation in mammalian cells. Nat Rev Genet 2:292–301.

Cremer T, Cremer M. 2010. Chromosome territories. Cold Spring Harb Perspect Biol 2:a003889.

Cross T, Griffiths G, Deacon E, Sallis R, Gough M, Watters D, Lord JM. 2000. PKC-delta is an apoptotic lamin kinase. Oncogene 19:2331–2337.

Dechat T, Pfleghaar K, Sengupta K, Shimi T, Shumaker DK, Solimando L, Goldman RD. 2008. Nuclear lamins: Major factors in the structural organization and function of the nucleus and chromatin. Genes Dev 22:832–853.

Dechat T, Gesson K, Foisner R. 2010a. Lamina-independent lamins in the nuclear interior serve important functions. Cold Spring Harb Symp Quant Biol 75:533–543.

Dechat T, Adam SA, Taimen P, Shimi T, Goldman RD. 2010b. Nuclear lamins. Cold Spring Harb Perspect Biol 2:a000547.

Dinant C, van Royen ME, Vermeulen W, Houtsmuller AB. 2008. Fluorescence resonance energy transfer of GFP and YFP by spectral imaging and quantitative acceptor photobleaching. J Microsc 231:97–104.

Dundr M, Hoffmann-Rohrer U, Hu Q, Grummt I, Rothblum LI, Phair RD, Misteli T. 2002. A kinetic framework for a mammalian RNA polymerase in vivo. Science 298:1623–1626.

Galiová G, Bártová E, Raška I, Krejčí J, Kozubek S. 2008. Chromatin changes induced by lamin A/C deficiency and the histone deacetylase inhibitor trichostatin A. Eur J Cell Biol 87:291–303.

Goldman AE, Moir RD, Montag-Lowy M, Stewart M, Goldman RD. 1992. Pathway of incorporation of microinjected lamin A into the nuclear envelope. J Cell Biol 119:725–735.

Goldman RD, Shumaker DK, Erdos MR, Eriksson M, Goldman AE, Gordon LB, Gruenbaum Y, Khuon S, Mendez M, Varga R, Collins FS. 2004. Accumulation of mutant lamin A causes progressive changes in nuclear architecture in Hutchinson–Gilford progeria syndrome. Proc Natl Acad Sci USA 101:8963–8968.

Holubcová Z, Matula P, Sedláčková M, Vinarský V, Doležalová D, Bárta T, Dvořák P, Hampl A. 2011. Human embryonic stem cells suffer from centrosomal amplification. Stem Cells 29:46–56.

Hozák P, Sasseville AM, Raymond Y, Cook PR. 1995. Lamin proteins form an internal nucleoskeleton as well as a peripheral lamina in human cells. J Cell Sci 108:635–644.

Kozlova N, Braga J, Lundgren J, Rino J, Young P, Carmo-Fonseca M, Visa N. 2006. Studies on the role of NonA in mRNA biogenesis. Exp Cell Res 312:2619–2630.

Lattanzi G, Columbaro M, Mattioli E, Cenni V, Camozzi D, Wehnert M, Santi S, Riccio M, Del Coco R, Maraldi NM, Squarzoni S, Foisner R, Capanni C. 2007. Pre-Lamin A processing is linked to heterochromatin organization. J Cell Biochem 102:1149–1159.

Lin F, Worman HJ. 1993. Structural organization of the human gene encoding nuclear lamin A and nuclear lamin C. J Biol Chem 268:16321–16326.

Lutz RJ, Trujillo MA, Denham KS, Wenger L, Sinensky M. 1992. Nucleoplasmic localization of prelamin A: Implications for prenylation-dependent lamin A assembly into the nuclear lamina. Proc Natl Acad Sci USA 89:3000–3004. Erratum in: Proc Natl Acad Sci USA 89:5699.

Malhas AN, Lee CF, Vaux DJ. 2009. Lamin B1 controls oxidative stress responses via Oct-1. J Cell Biol 184:45–55.

Malhas AN, Vaux DJ. 2009. Transcription factor sequestration by nuclear envelope components. Cell Cycle 8:959–960.

Malhas AN, Vaux DJ. 2011. The nuclear envelope and its involvement in cellular stress responses. Biochem Soc Trans 39:1795–1798.

McNamara LE, Burchmore R, Riehle MO, Herzyk P, Biggs MJ, Wilkinson CD, Curtis AS, Dalby MJ. 2012. The role of microtopography in cellular mechanotransduction. Biomaterials 33:2835–2847.

Meaburn KJ, Misteli T. 2007. Cell biology: Chromosome territories. Nature 445:379–781.

Neri LM, Raymond Y, Giordano A, Capitani S, Martelli AM. 1999. Lamin A is part of the internal nucleoskeleton of human erythroleukemia cells. J Cell Physiol 178:284–295.

Nikolova V, Leimena C, McMahon AC, Tan JC, Chandar S, Jogia D, Kesteven SH, Michalicek J, Otway R, Verheyen F, Rainer S, Stewart CL, Martin D, Feneley MP, Fatkin D. 2004. Defects in nuclear structure and function promote dilated cardiomyopathy in lamin A/C-deficient mice. J Clin Invest 113:357–369.

Orlova DY, Stixová L, Kozubek S, Gierman HJ, Šustáčková G, Chernyshev AV, Medvedev RN, Legartová S, Versteeg R, Matula P, Stoklasa R, Bártová E. 2012. Arrangement of nuclear structures is not transmitted through mitosis but is identical in sister cells. J Cell Biochem 113:3313–3329.

Ottaviano Y, Gerace L. 1985. Phosphorylation of the nuclear lamins during interphase and mitosis. J Biol Chem 260:624–632.

Peter M, Kitten GT, Lehner CF, Vorburger K, Bailer SM, Maridor G, Nigg EA. 1989. Cloning and sequencing of cDNA clones encoding chicken lamins A and B1 and comparison of the primary structures of vertebrate A- and B-type lamins. J Mol Biol 208:393–404.

Piston DW, Kremers GJ. 2007. Fluorescent protein FRET: The good, the bad and the ugly. Trends Biochem Sci 32:407–414.

Razin SV, Gromova II. 1995. The channels model of nuclear matrix structure. Bioessays 17:443–450.

Reddy S, Comai L. 2012. Lamin A, farnesylation and aging. Exp Cell Res 318:1–7.

Redwood AB, Gonzalez-Suarez I, Gonzalo S. 2011a. Regulating the levels of key factors in cell cycle and DNA repair: New pathways revealed by lamins. Cell Cycle 10:3652–3657.

Redwood AB, Perkins SM, Vanderwaal RP, Feng Z, Biehl KJ, Gonzalez-Suarez I, Morgado-Palacin L, Shi W, Sage J, Roti-Roti JL, Stewart CL, Zhang J, Gonzalo S. 2011b. A dual role for A-type lamins in DNA double-strand break repair. Cell Cycle 10:2549–2560.

Scaffidi P, Misteli T. 2006. Lamin A-dependent nuclear defects in human aging. Science 312:1059–1063.

Scaffidi P, Misteli T. 2008. Lamin A-dependent misregulation of adult stem cells associated with accelerated ageing. Nat Cell Biol 10:452–459.

Shimi T, Pfleghaar K, Kojima S, Pack CG, Solovei I, Goldman AE, Adam SA, Shumaker DK, Kinjo M, Cremer T, Goldman RD. 2008. The A- and B-type nuclear lamin networks: Microdomains involved in chromatin organization and transcription. Genes Dev 22:3409–3421.

Shumaker DK, Dechat T, Kohlmaier A, Adam SA, Bozovsky MR, Erdos MR, Eriksson M, Goldman AE, Khuon S, Collins FS, Jenuwein T, Goldman RD. 2006. Mutant nuclear lamin A leads to progressive alterations of epigenetic control in premature aging. Proc Natl Acad Sci USA 103:8703–8708.

Simon DN, Wilson KL. 2011. The nucleoskeleton as a genome-associated dynamic "network of networks." Nat Rev Mol Cell Biol 12:695–708.

Stixová L, Matula P, Kozubek S, Gombitová A, Cmarko D, Raška I, Bártová E. 2012. Trajectories and nuclear arrangement of PML bodies are influenced by A-type lamin deficiency. Biol Cell 104:418–432.

Sullivan T, Escalante-Alcalde D, Bhatt H, Anver M, Bhat N, Nagashima K, Stewart CL, Burke B. 1999. Loss of A-type lamin expression compromises nuclear envelope integrity leading to muscular dystrophy. J Cell Biol 147:913–920.

Sun Y, Booker CF, Kumari S, Day RN, Davidson M, Periasamy A. 2009. Characterization of an orange acceptor fluorescent protein for sensitized spectral fluorescence resonance energy transfer microscopy using a white-light laser. J Biomed Opt 14:054009.

Šustáčková G, Legartová S, Kozubek S, Stixová L, Pacherník J, Bártová E. 2012. Differentiation-independent fluctuation of pluripotency-related transcription factors and other epigenetic markers in embryonic stem cell colonies. Stem Cells Dev 21:710–720.

Tang CW, Maya-Mendoza A, Martin C, Zeng K, Chen S, Feret D, Wilson SA, Jackson DA. 2008. The integrity of a lamin-B1-dependent nucleoskeleton is a fundamental determinant of RNA synthesis in human cells. J Cell Sci 121:1014–1024.

Taniura H, Glass C, Gerace L. 1995. A chromatin binding site in the tail domain of nuclear lamins that interacts with core histones. J Cell Biol 131:33–44.

Vlcek S, Foisner R. 2007. Lamins and lamin-associated proteins in aging and disease. Curr Opin Cell Biol 19:298–304.

Vorburger K, Lehner CF, Kitten GT, Eppenberger HM, Nigg EA. 1989. A second higher vertebrate B-type lamin. cDNA sequence determination and in vitro processing of chicken lamin B2. J Mol Biol 208:405–415.

Wiesel N, Mattout A, Melcer S, Melamed-Book N, Herrmann H, Medalia O, Aebi U, Gruenbaum Y. 2008. Laminopathic mutations interfere with the assembly, localization, and dynamics of nuclear lamins. Proc Natl Acad Sci USA 105:180–185.

Worman HJ, Courvalin JC. 2004. How do mutations in lamins A and C cause disease? J Clin Incest 113:349–351.

Zhang YQ, Sarge KD. 2008. Sumoylation regulates lamin A function and is lost in lamin A mutants associated with familial cardiomyopathies. J Cell Biol 182:35–39.

SUPPORTING INFORMATION

Additional supporting information may be found in the online version of this article at the publisher's web-site.